Desalination and Water Treatment
www.deswater.com

doi: 10.1080/19443994.2015.1101712

57 (2016) 20027–20036
September

Taylor & Francis
Taylor & Francis Group

Application of response surface methodology for electrochemical oxidation of the C.I. Reactive Orange 7 using flow reactor with Ti/Sb–SnO_2 anode

Jalal Basiri Parsa*, Mansoureh Bahiraei, Farideh Nabizadeh Chianeh*

Faculty of Chemistry, Department of Applied Chemistry, University of Bu-Ali Sina, Hamadan, Iran, Tel. +98 81 318282807; Fax: +98 81 318257407; emails: parssa@basu.ac.ir (J. Basiri Parsa), Sh.sooreh_b@yahoo.com (M. Bahiraei), Nabizadeh_farideh@yahoo.com (F. Nabizadeh Chianeh)

Received 12 December 2014; Accepted 26 September 2015

ABSTRACT

In this work, the electrochemical oxidation of the C.I. Reactive Orange 7 was investigated with Ti/Sb–SnO_2 electrode as anode using a flow reactor in two modes: circulating and continuous. The Ti/Sb-SnO_2 anode was prepared using dip-coating and thermal decomposition method, and then it was characterized by scanning electron microscopy, cyclic voltammetry, and energy dispersive spectrometer. The parameters such as current density, flow rate, temperature and time for the circulating mode, and current density and flow rate for the continuous mode were selected as independent variables in central composite design, while the color removal efficiency was considered as the response function for two modes. In optimum conditions, color removal efficiency for the circulating and the continuous modes were 99.97 and 90.91%, respectively.

Keywords: Electrochemical oxidation; Reactive Orange 7; Flow reactor; Ti/Sb–SnO_2 anode; Central composite design (CCD)

1. Introduction

Synthetic dyes are a group of organic compounds that are widely used in textile industries. These industries consume large volumes of water and produce colored wastewater during dyeing process. The presence of stable synthetic dyes in water prevent from sun light penetration, and threat living organism [1]. Hence, for reduction of environmental effect of colored wastewater, the application of new treating methods is necessary. There are several methods for the textile wastewater treatment such as photo-catalytic method [2], biological treatment [3], ozonation [4], sonication [5], physicochemical methods [6,7], enzymatic treatments [8], and electrochemical techniques [9].

The biological treatments are commonly the most efficient and economic for most textile effluents but they are inefficient and time-consuming. The physicochemical methods are efficient for decolorization, but they are expensive and lead to a high amount of sludge [7]. Ozonation is a powerful technique for wastewater decolorization, but it is very costly [10].

In electrochemical oxidation, pollutants can be removed by two ways: (i) directly, when the organic compounds are oxidized by direct electron transfer to the electrode surface and, (ii) indirectly, when electrons are transferred to other electroactive species such as hypochlorite/chlorine and hydrogen peroxide. This method can effectively oxidize many organic and

*Corresponding authors.

inorganic pollutants into CO_2 and H_2O. This technology has several advantages such as: its strong oxidation performance, a fast reaction rate, simple operation, safety, one-time electrolyte addition, environmental compatibility, and cost effectiveness [11,12]. In the electrochemical methods, the proper choice of electrode materials and reactor is very important [13]. The oxidation of organic molecules occurs in small layer near electrode surface; thus, flow reactor is used in order to eliminate mass transfer limitation [1,14]. Dimensionally stable anodes (DSAs) that are formed by thermal decomposition of organic salts on Ti support are found to have varying degree of success for electrochemical oxidation treatment. DSAs are classified as active and non-active. In active mode, the oxidation of organic species is performed by the formation of higher oxidation state oxides of the metals. In non-active mode, there is no higher oxidation state and the oxidation of organic species is performed by an adsorbed hydroxyl radical [14–16].

In this study, in order to investigate the electrochemical oxidation of Reactive Orange 7 by Ti/Sb–SnO_2, flow reactor was used in two modes: circulating and continuous. The Ti/Sb–SnO_2 electrode was prepared using dip-coating and thermal decomposition method. This electrode has been widely investigated to degrade different organic pollutants and it has several advantages, such as; high efficiency for the electro-catalytic oxidation of organic pollutions, high chemical and electrochemical stability as a consequence of the rather large band gap, high electrical conductivity, high oxygen evolution over potential, and easy preparation [12,17–19]. Optimization of effective parameters in color removal efficiency including; flow rate, current density, temperature, and time in the circulating mode, and flow rate and current density in the continuous mode were performed using response surface methodology (RSM).

2. Experimental

2.1. Materials

All chemicals, including $SbCl_3$ (99.5%, Sigma Aldrich), $SnCl_4{\cdot}5H_2O$ (98%, Sigma Aldrich), HCl (Merck) and ethanol (98%, Merck) were used without further purification. The Reactive Orange 7 dye (RO7), $C_{20}H_{17}N_3Na_2O_{11}S_3$, was obtained from Alvan Sabet Company (Iran). The structure of RO7 (M_W617.537 g/mol; λ_{max} 480 nm) is given in Fig. 1. Sodium chloride (produced by Merck Company) was used as supporting electrolyte in all experiments. Other reagents, used in study, were of analytical grade. Deionized water was used for the preparation

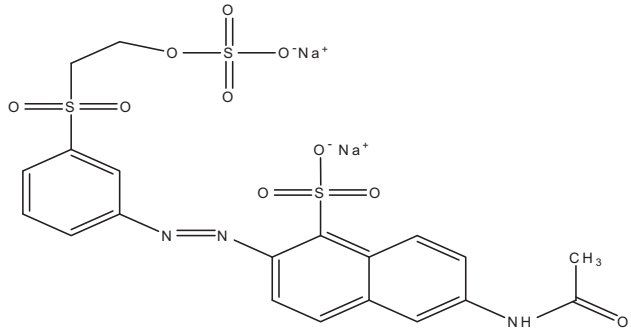

Fig. 1. Chemical structure of Reactive Orange 7 (RO7).

of all solutions. Experiments were carried out using a Ti/Sb–SnO_2 (2 cm × 2 cm) as anode and a stainless steel cathode (3 cm × 3 cm).

2.2. Electrode preparation

Titanium (Ti) meshes (2 cm × 2 cm) were immersed into 40 wt% NaOH solution at 60˚C for 1 h, in 15 wt% oxalic acid at 95˚C for another 1 h, and then were rinsed by deionized water. In the next step, the electrodes were prepared by dip-coating and thermal decomposition method using a solution containing $SnCl_4{\cdot}5H_2O$ and $SbCl_3$ (with molar ratio of Sn: Sb = 98.5:1.5) dissolved in 99.8% ethanol, finally concentrated HCl was added drop-by-drop until the solution was clear. Solution was kept under ultrasonic for 2 h. The Ti meshes were put into solution for 2 min, dried for solvent evaporation in an oven at 95˚C for 10 min, and then placed into preheated furnace at 500˚C for 20 min. This procedure (dipping, drying, and pyrolysis) was repeated 15 times. Electrodes were weighed after each coating. Finally, the electrodes were annealed at 500˚C for 1 h in a muffle furnace [13,20,21].

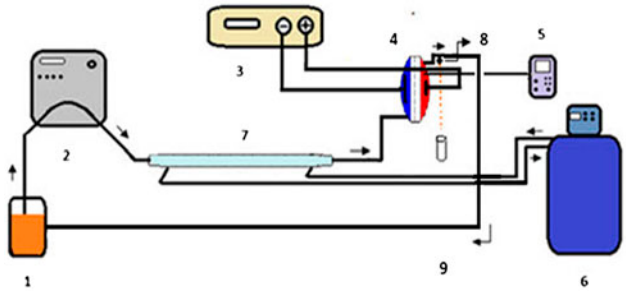

Fig. 2. Experimental setup.
Notes: (1) reservoir, (2) pump, (3) D.C. power supply, (4) flow cell, (5) the thermometer, (6) refrigerated bath circulator, (7) thermal exchanger, (8) valve, (For continuous mode, stream (9) will be absent).

Table 1
Range of the independent variables used in the experimental design in the circulating mode

Independent variables	Levels				
	−α	−1	0	+1	+α
Current density, X_1 (mA cm^{-2})	2.93	5	10	15	17.07
Flow rate, X_2 (mL min^{-1})	28.79	35	50	65	71.21
Temperature, X_3 (℃)	10.86	15	25	35	39.15
Time, X_4 (min)	6.89	10	17.50	25	28.11

Table 2
Range of the independent variables used in the experimental design in the continuous mode

Independent variables	Levels				
	−α	−1	0	+1	+α
Current density, X_1 (mA cm^{-2})	2.93	5	10	15	17.07
Flow rate, X_2 (mL min^{-1})	28.79	35	50	65	71.21

2.3. Reactor set up and experimental procedure

The electrochemical flow reactor system was conducted in two modes: (i) circulating and (ii) continuous. Fig. 2 gives the schematic diagram of the flow reactor. It consists of a Ti/Sb–SnO_2 (2 cm × 2 cm) as anode and steel stainless (3 cm × 3 cm) as cathodes that are connected to a power supply in order to supply a constant current. The anode and cathode are fixed with an inter-electrode gap of 1.5 cm. The volume of reactor is 200 mL. The inlet and outlet of reactor are connected to a reservoir (500 mL) using silicon rubber tubes. The setup can operated both in circulating and continuous modes.

Table 3
CCD matrix for electrochemical oxidation of the Reactive Orange 7 dye and predicted and observed color removal efficiencyin the circulating mode

Exp	X_1 (mA/cm^2)	X_2 (mL/min)	X_3 (℃)	X_4 (minute)	Color removal %	
					Predicted	Observed
1	15.00	65.00	35.00	25.00	96.57	98.94
2	5.00	35.00	15.00	25.00	94.16	93.06
3	10.00	50.00	25.00	17.50	97.49	97.42
4	5.00	35.00	35.00	10.00	46.49	46.31
5	10.00	71.21	25.00	17.50	100.91	98.26
6	10.00	50.00	39.14	17.50	98.11	98.90
7	5.00	35.00	15.00	10.00	41.10	37.75
8	15.00	65.00	15.00	25.00	100.21	98.97
9	10.00	50.00	25.00	17.50	97.49	97.26
10	10.00	50.00	25.00	17.50	97.49	97.62
11	5.00	65.00	35.00	25.00	100.24	98.75
12	5.00	35.00	35.00	25.00	99.55	96.66
13	15.00	35.00	15.00	25.00	99.52	99.00
14	15.00	35.00	15.00	10.00	88.21	92.87
15	15.00	35.00	35.00	10.00	84.57	84.20
16	15.00	65.00	35.00	10.00	93.56	93.73
17	10.00	28.79	25.00	17.50	94.07	98.50
18	10.00	50.00	25.00	6.86	58.93	55.12
19	10.00	50.00	10.86	17.50	96.87	98.35
20	10.00	50.00	25.00	17.50	97.49	97.59
21	15.00	35.00	00 35	25.00	95.88	98.50
22	5.00	65.00	15.00	10.00	50.09	50.15
23	5.00	65.00	35.00	10.00	55.48	59.61
24	2.93	50.00	25.00	17.50	73.10	74.84
25	15.00	65.00	15.00	10.00	97.20	98.62
26	17.07	50.00	25.00	17.50	103.81	98.18
27	10.00	50.00	25.00	28.11	98.58	98.50
28	5.00	65.00	15.00	25.00	94.86	98.35
29	10.00	50.00	25.00	17.50	97.49	97.73
30	10.00	50.00	25.00	17.50	97.49	93.27

2.4. Experimental design and optimization

To investigate and find the optimum conditions for electrochemical oxidation of RO7 in a flow reactor, a central composite design (CCD) model based on four factors for the circulating mode and two factors for continuous mode was used as experimental design model. The independent variables were current density (X_1), flow rate (X_2), temperature (X_3), and time (X_4) for circulating mode, and current density (X_1) and flow rate (X_2) for the continuous mode. This design requires an experiment number according to $N = 2^k + 2k + C_0$, where k is the number of factor and C_0 is the number of central point [2,22]. The ranges of variables were selected based on the literature values and results of preliminary experiments [9]. Tables 1 and 2 show the ranges and the levels of these variables for circulating mode and continuous mode, respectively.

Total number of experiments in this study was 30 and 13, with 5 and 6 replicates at the design center for continuous and circulating modes, respectively. All the experiments were carried out in random order to avoid systematic error. The behavior of the systems can be explained by the quadratic equation:

$$Y = \beta_0 + \sum_{j=1}^{k} \beta_j x_j + \sum_{j=1}^{k} \beta_{jj} x_j^2 + \sum_{i} \sum_{<j=2}^{k} \beta_{ij} x_i x_j + e_i \quad (1)$$

where Y is the response, k is the number of factors, x_i and x_j are variables, β_0 is the constant coefficient, β_j, β_{jj}, and β_{ij} are interaction coefficients of linear, quadratic, and the second-order terms, respectively, and e_i is the error.

Table 4
CCD matrix for electrochemical oxidation of the Reactive Orange 7 dye and predicted and observed color removal efficiency in the continuous mode

			Color removal %	
Exp	X_1 (mA/cm^2)	X_2 (mL/min)	Predicted	Observed
1	10.00	50.00	39.36	45.12
2	10.00	50.00	39.36	37.12
3	10.00	50.00	39.36	36.65
4	10.00	50.00	39.36	38.65
5	10.00	50.00	39.36	38.94
6	10.00	71.21	17.61	15.49
7	10.00	28.79	71.22	76.51
8	15.00	35.00	96.65	90.77
9	2.93	50.00	09.19	08.40
10	15.00	65.00	26.54	25.90
11	5.00	65.00	17.98	20.70
12	17.07	50.00	66.83	70.79
13	5.00	35.00	23.69	21.16

The Design-Expert 8.0 software was used to make regression for regression analysis of experimental data and to obtain the interaction between the experiments variables and the response. For optimization, a model in Design Expert software was searched for a combination of factor levels that simultaneously satisfy the requirements placed on each of the responses and

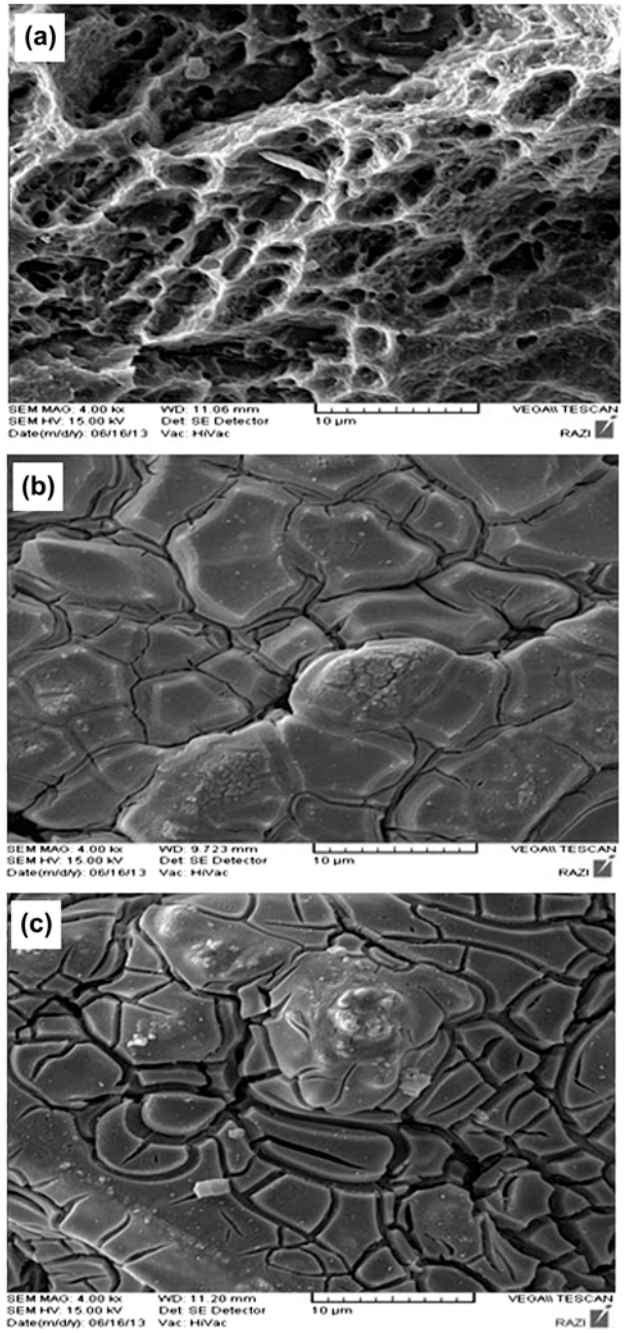

Fig. 3. SEM images of (a) Ti electrode without coating, (b) Ti/Sb-SnO_2 electrode fresh, and (c) Ti/Sb-SnO_2 after being used for electrolysis for 15 h.

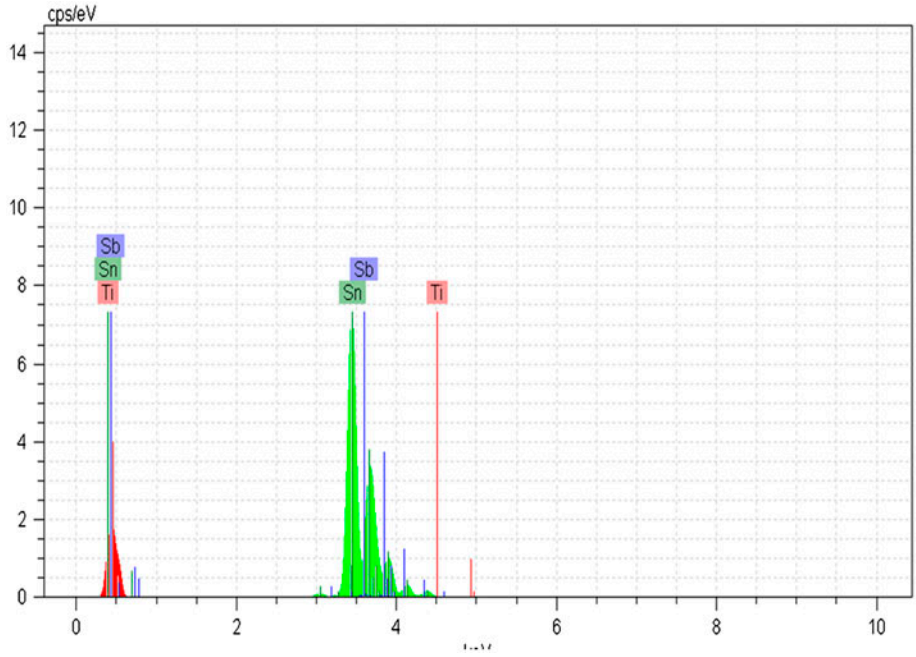

Fig. 4. EDS analysis of the coating surfaces a Ti/Sb-SnO_2 electrode.

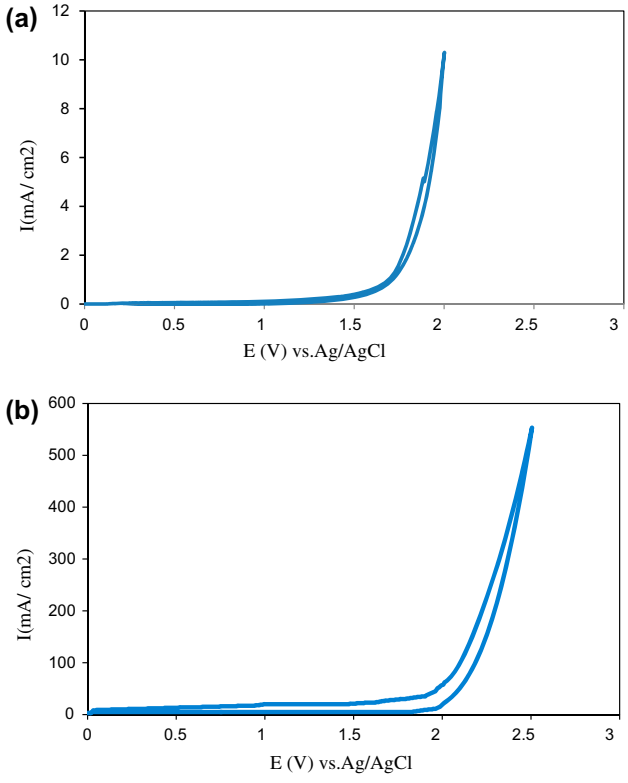

Fig. 5. Cyclic voltamograms obtained from different electrodes after reaching steady states: (a) Ti net and (b) Ti/Sb-SnO_2.

factors. The targets were selected as maximum color removal percent at within parameter range [8,23].

2.5. Analysis

Before conducting each experiment, flow rate, temperature, and current density were adjusted according to Tables 3 and 4 by pump (ISMATEC, 404B), Refrigerated Bath Circulator (LabTech, LCB-RO8), and D.C. power supply, respectively. At intervals proposed in Tables 3 and 4, 3 mL of sample was taken from the electrochemical reactor. The solution color was analyzed at 480 nm by the UV–visible spectrophotometer (JASCO. v-630, Japan), then the concentration of dye in different solution and color removal efficiency was determined using the calibration curve and the following equation [24]:

$$\text{Color Removal}\,\% = ((C_0 - C)/C_0) \times 100 \quad (2)$$

In this equation, C_0 and C are initial and final concentration of dye in the synthetic wastewater.

3. Results and discussion

3.1. Characterization of Ti/Sb-SnO_2

3.1.1. Surface morphology

Scanning Electron Microscopy (SEM) was used for investigation of Ti/Sb–SnO_2 surface morphology by a

Table 5
ANOVA result of the quadratic models for color removal efficiencyin the circulating mode

Sources of variation	Sum of squares	Degree of freedom	Mean square	*F*-value	Prob. > *F*	
Model	9,682.20	9	1,075.80	114.88	<0.0001	Significant
Lack of fit	172.07	15	11.47	3.77	0.0749	Not significant
Pure error	15.22	5	3.04			
Residual	187.29	20	9.36			
Core total	9,869.48	29				

VEGA//TESCAN. The SEM images of the electrodes before and after coating are shown in Fig. 3(a) and (b). It can be observed in the images that surface coverage of electrode and active sites are increased with presence of Sb–SnO_2 [25]. A substantial amount of cracks can be seen in the oxide film, which can be attributed to the contraction of the hydroxide coating layer during drying and calcinations of the electrode [26].

In order to examine the stability of the electrode in high anodic potential, a SEM of electrode was taken after being used for electrochemical oxidation of RO7 for 15 h (See Fig. 3(c)). Comparison of SEM images (See Fig. 3(b) and (c)) shown that little change occurred in surface of the electrode after 15 h of electrolysis. Also, the results show that columbic efficiency was almost fixed after 15 h in all conditions [25].

The elemental compositions of the coating were analyzed by Energy Dispersive Spectrometer (EDS) (See Fig. 4). The result of EDS confirmed the presence of Sb, Sn, and Ti in the electrode.

3.1.2. Cyclic voltammetry

Cyclic voltammetry (CV) was performed at 50 mV s^{-1} in 1 M H_2SO_4 solution at room temperature. The cyclic voltamograms of the Ti substrate and Ti/Sb–SnO_2 anode are shown in Fig. 5(a) and (b), respectively. The onset potential was 1.85 V vs. Ag/AgCl in Ti/Sb–SnO_2 as anode electrode and it was much higher than the typical value expected for oxygen evolution in acid solution which is 1.02 V vs. Ag/AgCl, indicating that oxygen evolution was kinetically suppressed [22]. The Ti and Ti/Sb–SnO_2 electrode have an onset potential of 1.5 V and 1.85 V vs. Ag/AgCl for O_2 evolution, respectively. The high onset potential for O_2 evolution is desired because O_2 evolution is a side reaction in the process of anodic oxidation of pollutants. Therefore, the much higher onset potential for O_2 evolution suggested that the Ti/Sb–SnO_2 may have much higher current efficiency than the Ti electrode for electrochemical oxidation RO7 [21]. Also, in the blank solution, no other peaks appeared in any of the cyclic voltamograms except the one formed by water discharge, indicating that the Ti/Sb–SnO_2 electrode surface is stable [20].

3.2. Optimization of electrochemical oxidation treatment of RO7

The quadratic Eqs. (3) and (4) describe the color removal efficiency in the circulating and the continuous modes, respectively. In these equations, non-significant coefficients were excluded based on the results of each mode analysis of variance (ANOVA):

$$\text{Color removal efficiency}\,(\%) = 97.49 + 2.43x_1 + 0.45x_2 + 10.85x_3 + 14.03x_4 - 2.06x_1x_4 - 2.27x_2x_3 - 10.45x_3x_4 - 4.51x_3^2 - 9.36x_4^2 \quad (3)$$

$$\text{Color removal efficiency}\,(\%) = 40.50 + 20.38x_1 - 18.95x_2 - 16.10x_1x_2 \quad (4)$$

Table 6
ANOVA result of the quadratic models for color removal efficiency in the continuous mode

Sources of variation	Sum of squares	Degree of freedom	Mean square	*F*-value	Prob. > *F*	
Model	7,233.41	3	2,411.27	111.96	<0.0001	Significant
Lack of fit	149.16	5	29.83	2.67	0.1813	Not significant
Pure error	44.68	4	11.17			
Residual	193.84	9	21.54			
Core total	7,427.65	12				

Statistical testing of the models was performed with the Fisher, s statistical test for ANOVA, as shown in Tables 5 and 6. The values of R^2 and R^2_{adj} are close to 1.0, which indicated a high correlation between the observed and the predicted values, as shown in Fig. 6(a) and (b) for recycle and flow modes, respectively. Models *F*-values are 114.88 and 71.74 for color removal efficiency of the recycle and flow modes, respectively, expressing these models are significant. In addition, the significance of each term in model is evaluated with *p*-value (prob. > *F*). If a *p*-value is less than 0.05, the term is significant at 95% of confidence level. The terms with $p > 0.05$ can be removed from models. However, in this study, the insignificant terms are retained to evaluating the effect of the terms and support the hierarchical nature of these models [23,27].

3.3. Determination of optimal condition for RO7

Optimized conditions under determined ranges were obtained, 10.50 mA cm^{-2} current density, 51.50 mL min^{-1} flow rate, 26℃ temperature, 18.25 min time for the circulating mode, and 14.23 mA cm^{-2} current density 35.13 mL min^{-1} flow rate for the continuous mode. Under these optimized conditions, 99.97 and 90.91% color removal efficiency were obtained for the circulating and the continuous modes, respectively. To confirm the optimum conditions, the experiments were performed under these conditions. In these experiments, 98.22 and 89.12% color removal efficiency were obtained for the circulating and the continuous modes, respectively [22,23].

3.4. Effect of operational parameters

All experiments were conducted under the 100 mg L^{-1} initial concentration of the dye solution, 1.5 g L^{-1} NaCl as an electrolyte and natural pH of the dye solution. At this pH (5.4), the predominant active chlorine are Cl_2 and HClO as given in Eqs. (5) and (6).

$$2Cl^-(aq) \rightarrow Cl_2(aq) + 2e^- \quad (5)$$

$$Cl_2(aq) + H_2O(l) \rightarrow HOCl\,(aq) + Cl^-(aq) + H^+(aq) \quad (6)$$

The response surface and counter plots for the color removal efficiency in the circulating mode are shown in Figs. 7(a) and (b), 8(a) and (b) and 9(a) and (b) as a function of the independent variables, current density, temperature, time, and flow rate.

Fig. 7(a) and (b) (data obtained at $X_3 = 25$℃ and $X_2 = 50$ mL min^{-1}) shows the color removal efficiency behavior as a function of current density and time. Clearly, the color removal efficiency increases with increase in current density. This may be due to the production of high amount of oxidant species such as OCl^-, $OH^\cdot$ and higher oxidation state oxides of metals, but with further increases in current density, chlorine generation is increased, and hence the direct anodic oxidation would be depressed. The indirect oxidation would be dominant in this mode. Consequently, the color removal efficiency would decrease with current density after the highest color removal efficiency [9].

Color removal efficiency behavior as a function of current density and temperature in Fig. 8(a) and (b) (data obtained at $X_2 = 50$ mL min^{-1} and $X_4 = 17.5$ min) clearly showed that the color removal efficiency increases with temperature in low current densities

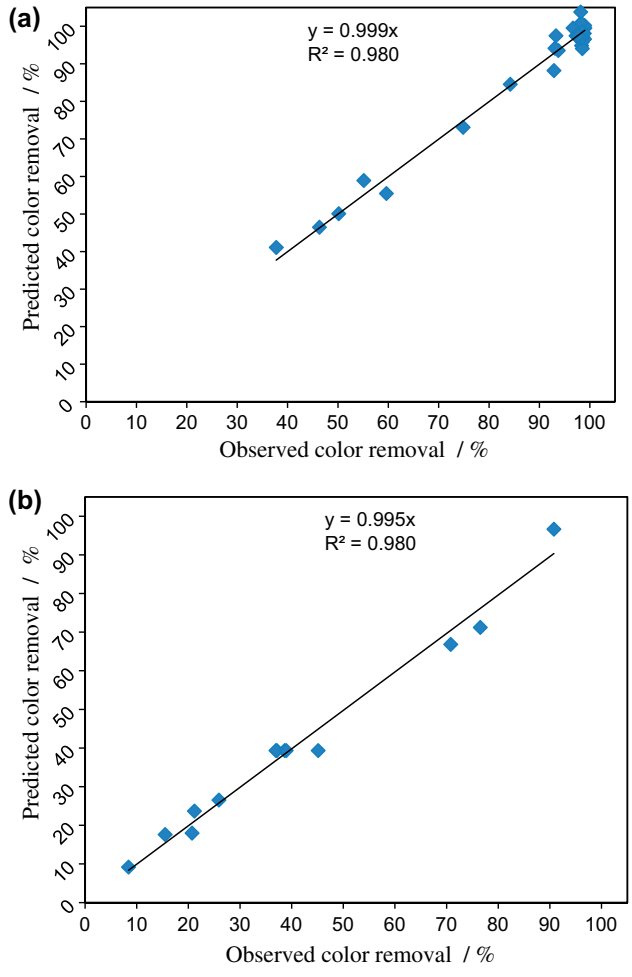

Fig. 6. Predicted and observed plot for color removal for the (a) circulating mode and (b) continuous mode.

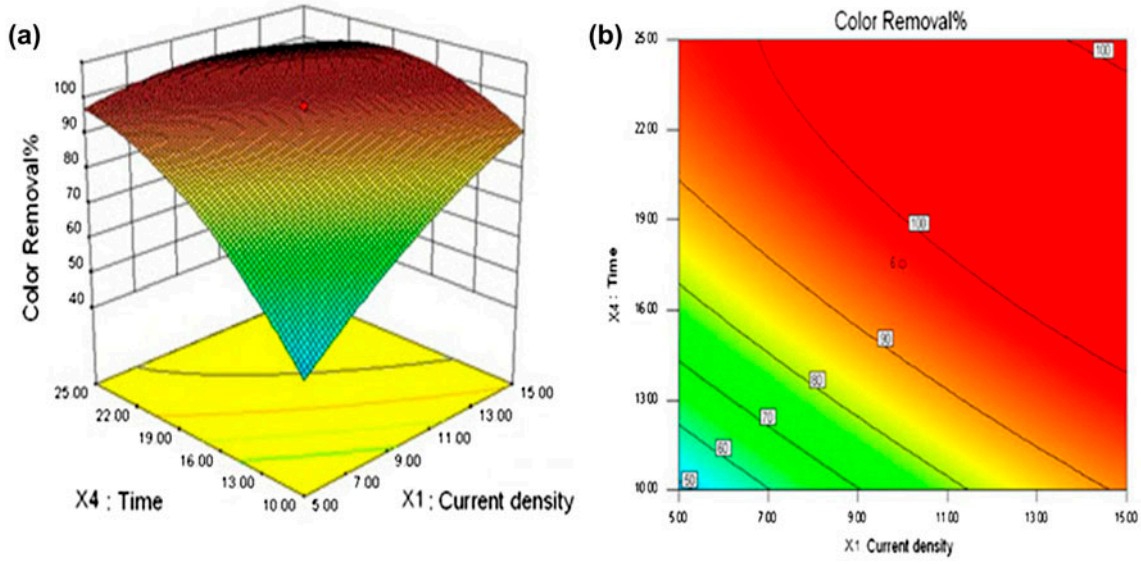

Fig. 7. Response surface (a) and counter plots (b) for color removal efficiency for the circulating mode as a function of current density and time (at X_3 = 25℃, using X_2 = 50 mL min^{-1}).

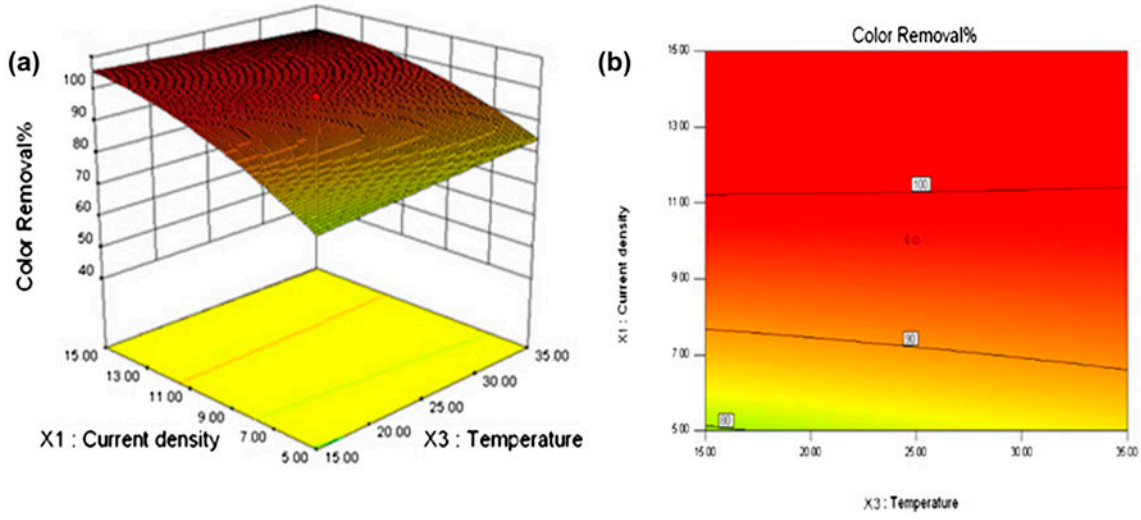

Fig. 8. Response surface (a) and counter plots (b) for color removal efficiency for the circulating mode as a function of current density and temperature (at X_2 = 50 mL min^{-1}, X_4 = 17.5 min).

due to an increase in the reaction rate and decreases with temperature in high current densities because the Cl_2 solubility is lower [10,14].

Fig. 9(a) and (b) shows the response surface and counter plots (data obtained at X_3 = 25℃ and using X_1 = 10 mA min^{-1}), of the color removal efficiency as a function of time and flow rate; as can be seen in Fig. 9(a) and (b), the best condition for color removal efficiency was attained at the highest time and flow rate, because color removal efficiency values are favored by the highest time and the dye solutions are in further contact with the anode in this mode.

The response surface and counter plots for the color removal efficiency in the continuous mode were investigated as a function of the independent variables, current density, and flow rate. Optimum temperature of circulating mode was used in the continuous mode to decrease consuming dye solution and chemical materials. In addition, the continuous mode is independent of time.

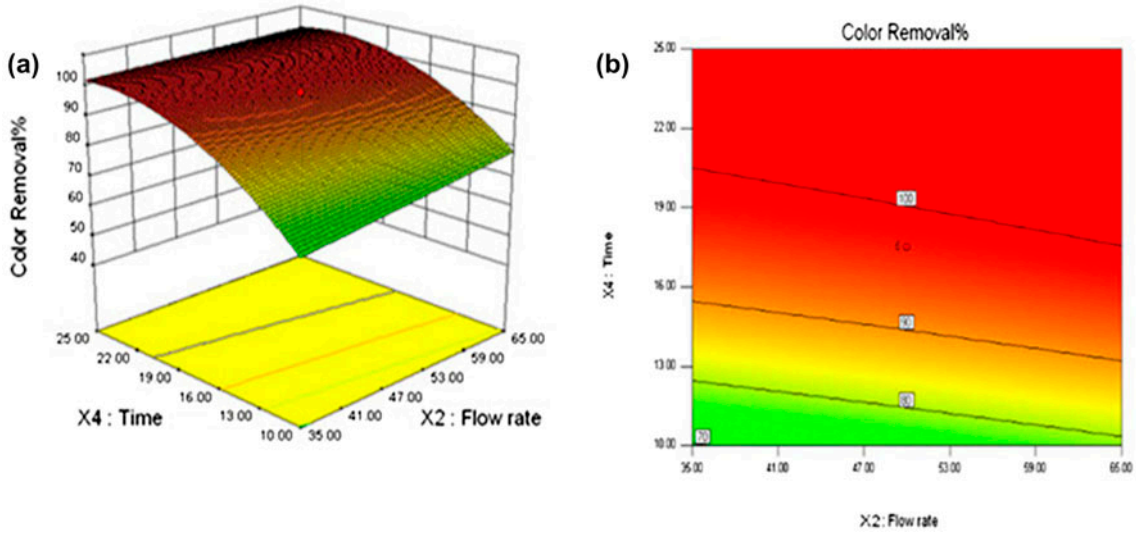

Fig. 9. Response surface (a) and counter plots (b) for color removal efficiency for the circulating mode as a function of time and flow rate (at X_3 = 25°C, using X_1 = 10 mA min^{-1}).

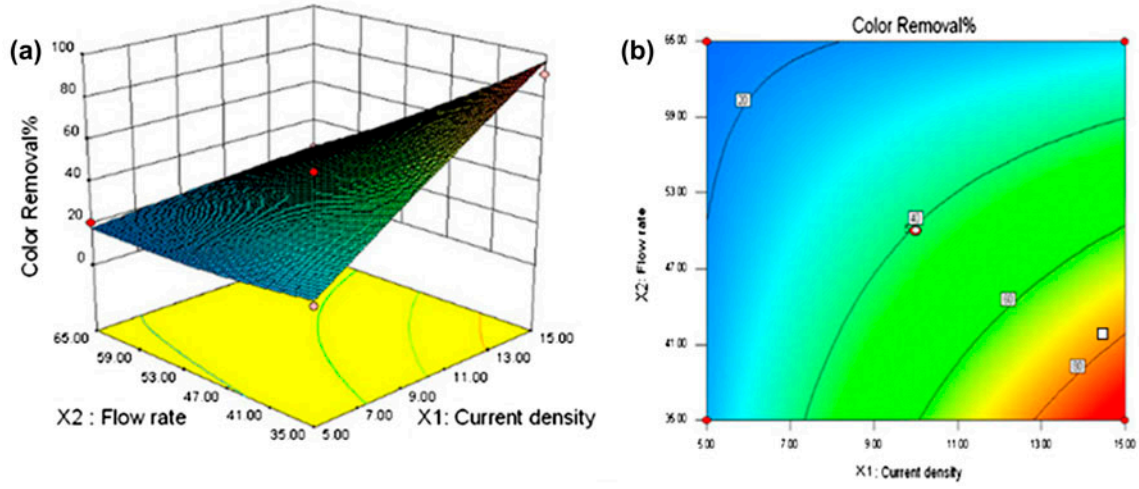

Fig. 10. Response surface (a) and counter plots (b) for color removal efficiency for the continuous mode as a function of current density and flow rate.

Fig. 10(a) and (b) shows the color removal efficiency as a function of current density and flow rate. The maximum color removal efficiency is attained at the highest current density and lowest flow rate because high amount of oxidants species such as OCl^-, $OH^\cdot$ and higher oxidation state oxides of the metals are produced in this mode.

4. Conclusions

The electrochemical oxidation RO7 was studied in the flow reactor in the circulating and the continuous modes with Ti/Sb–SnO_2 electrode as anode. Ti/Sb–SnO_2 anode has good stability in high anodic potential and high onset potential for O_2 evolution. Using the RSM can be many numbers of variables that affect the process to be modeled and investigated. The fit of the models was checked by the determination of coefficient (R^2). The optimum condition for the highest color removal efficiency of RO7 solution in circulating mode (99.97%) attained at 10.50 mA cm^{-2} current density, 51.50 mL min^{-1} flow rate, 26°C temperature and 18.25 min; while in continuous mode (90.91%) 14.23 mA cm^{-2} current density and 35.13 mL min^{-1}

flow rate. These results indicate that these methods can be used for decolorization of dyes present in the effluent of textile industries.

Acknowledgments

The authors thank the University of Bu-Ali Sina, Iran for financial and other supports.

References

[1] J.M. Aquino, R.C. Rocha-Filho, N. Bocchi, S.R. Biaggio, Electrochemical degradation of the Acid Blue 62 dye on a β-PbO_2 anode assessed by the response surface methodology, J. Appl. Electrochem. 40 (2010) 1751–1757.
[2] A.R. Khataee, M.B. Kasiri, L. Alidokht, Application of response surface methodology in the optimization of photocatalytic removal of environmental pollutants using nanocatalysts, Environ. Technol. 32 (2011) 1669–1684.
[3] J. Cha, S. Choi, H. Yu, H. Kim, C. Kim, Directly applicable microbial fuel cells in aeration tank for wastewater treatment, Bioelectrochemistry 78 (2010) 72–79.
[4] J.B. Parsa, M. Abbasi, A. Cornell, Improvement of the current efficiency of the Ti/Sn-Sb-Ni oxide electrode via carbon nanotubes for ozone generation, J. Electrochem. Soc. 159 (2012) 265–269.
[5] P. Foladori, B. Laura, A. Gianni, Z. Giuliano, Effects of sonication on bacteria viability in wastewater treatment plants evaluated by flow cytometry—Fecal indicators, wastewater and activated sludge, Water Res. 41 (2007) 235–243.
[6] A.H. Essadki, B. Gourich, C. Vial, H. Delmas, M. Bennajah, Defluoridation of drinking water by electrocoagulation/electroflotation in a stirred tank reactor with a comparative performance to an external-loop airlift reactor, J. Hazard. Mater. 168 (2009) 1325–1333.
[7] J.B. Parsa, F.N. Chianeh, Evaluation of electro-coagulation method for decolorization and degradation of organic dyes in aqueous solutions, Korean J. Chem. Eng. 29 (2012) 1585–1590.
[8] K. Murugesan, A. Dhamija, I.-H. Nam, Y.-M. Kim, Y.-S. Chang, Decolourization of reactive black 5 by laccase: Optimization by response surface methodology, Dyes Pigm. 75 (2007) 176–184.
[9] H. Zhang, Y. Li, X. Wu, Y. Zhang, D. Zhang, Application of response surface methodology to the treatment landfill leachate in a three-dimensional electrochemical reactor, Waste Manage. 30 (2010) 2096–2102.
[10] J.M. Aquino, R.C. Rocha-Filho, N. Bocchi, S.R. Biaggio, Electrochemical degradation of the Reactive Red 141 dye on a β-PbO_2 anode assessed by the response surface methodology, J. Braz. Chem. Soc. 21 (2010) 324–330.
[11] H. Lin, J. Niu, J. Xu, H. Huang, D. Li, Z. Yue, C. Feng, Highly efficient and mild electrochemical mineralization of long-chain perfluorocarboxylic acids (C9–C10) by Ti/SnO_2–Sb–Ce, Ti/SnO_2–Sb/Ce–PbO_2, and Ti/BDD electrodes, Environ. Sci. Technol. 47 (2013) 13039–13046.
[12] L. Zhang, L. Xu, J. He, J. Zhang, Preparation of Ti/SnO_2-Sb electrodes modified by carbon nanotube for anodic oxidation of dye wastewater and combination with nanofiltration, Electrochim. Acta 117 (2014) 192–201.
[13] H. Xu, A. Li, X. Cheng, Electrochemical performance of doped SnO2 coating on Ti base as electrooxidation anode, Int. J. Electrochem. Sci. 6 (2011) 5114–5124.
[14] G.F. Pereira, R.C. Rocha-Filho, N. Bocchi, S.R. Biaggio, Electrochemical degradation of bisphenol A using a flow reactor with a boron-doped diamond anode, Chem. Eng. J. 198–199 (2012) 282–288.
[15] C.A. Basha, J. Sendhil, K.V. Selvakumar, P.K.A. Muniswaran, C.W. Lee, Electrochemical degradation of textile dyeing industry effluent in batch and flow reactor systems, Desalination 285 (2012) 188–197.
[16] A.R. Zeradjanin, F.L. Mantia, J. Masa, W. Schuhmann, Utilization of the catalyst layer of dimensionally stable anodes—Interplay of morphology and active surface area, Electrochim. Acta 82 (2012) 408–414.
[17] H. Lin, J. Niu, S. Ding, L. Zhang, Electrochemical degradation of perfluorooctanoic acid (PFOA) by Ti/SnO_2–Sb, Ti/SnO_2–Sb/PbO_2 and Ti/SnO_2–Sb/MnO_2 anodes, Water Res. 46 (2012) 2281–2289.
[18] J. Niu, Y. Bao, Y. Li, Z. Chai, Electrochemical mineralization of pentachlorophenol (PCP) by Ti/SnO_2–Sb electrodes, Chemosphere 92 (2013) 1571–1577.
[19] A.I. del Río, J. Fernández, J. Molina, J. Bonastre, F. Cases, On the behaviour of doped SnO2 anodes stabilized with platinum in the electrochemical degradation of reactive dyes, Electrochim. Acta 55 (2010) 7282–7289.
[20] J. Kong, S. Shi, X. Zhu, J. Ni, Effect of Sb dopant amount on the structure and electrocatalytic capability of Ti/Sb-SnO_2 electrodes in the oxidation of 4-chlorophenol, J. Environ. Sci. 19 (2007) 1380–1386.
[21] J.B. Parsa, Z. Merati, M. Abbasi, Modeling and optimization of electrochemical oxidation of C.I Reactive Orange 7 on the Ti/Sb-SnO_2 as anode via response surface methodology, J. Ind. Eng. Chem. 19 (2013) 1350–1355.
[22] B.K. Körbahti, A. Tanyolaç, Electrochemical treatment of simulated textile wastewater with industrial components and Levafix Blue CA reactive dye: Optimization through response surface methodology, J. Hazard. Mater. 151 (2008) 422–431.
[23] B.K. Körbahti, N. Aktaş, A. Tanyolaç, Optimization of electrochemical treatment of industrial paint wastewater with response surface methodology, J. Hazard. Mater. 148 (2007) 83–90.
[24] J.B. Parsa, M. Abbasi, Application of *in situ* electrochemically generated ozone for degradation of anthraquninone dye Reactive Blue 19, J. Appl. Electrochem. 42 (2012) 435–442.
[25] J. Basiriparsa, M. Abbasi, High-efficiency ozone generation via electrochemical oxidation of water using Ti anode coated with Ni–Sb–SnO_2, J. Solid State Electrochem. 16 (2012) 1011–1018.
[26] J.-J. Jow, H.-H. Lai, H.-R. Chen, C.-C. Wang, M.-S. Wu, T.-R. Ling, Effect of hydrothermal treatment on the performance of RuO_2–Ta_2O_5/Ti electrodes for use in supercapacitors, Electrochim. Acta 55 (2010) 2793–2798.
[27] Y. Zheng, Y. Liu, A. Wang, Fast removal of ammonium ion using a hydrogel optimized with response surface methodology, Chem. Eng. J. 171 (2011) 1201–1208.